

Scaling behavior in turbulent Rayleigh-Bénard convection revealed by conditional structure functions

Emily S. C. Ching,^{*} Yue-Kin Tsang,[†] and T. N. Fok*Department of Physics, The Chinese University of Hong Kong, Shatin, Hong Kong*

Xiaozhou He and Penger Tong

Department of Physics, Hong Kong University of Science and Technology, Clear Water Bay, Kowloon, Hong Kong

(Received 4 February 2012; published 3 January 2013)

We show that the nature of the scaling behavior can be revealed by studying the conditional structure functions evaluated at given values of the locally averaged thermal dissipation rate. These conditional structure functions have power-law dependence on the value of the locally averaged thermal dissipation rate, and such dependence for the Bolgiano-Obukhov scaling is different from the other scaling behaviors. Our analysis of experimental measurements verifies the power-law dependence and reveals the Bolgiano-Obukhov scaling behavior at the center of the bottom plate of the convection cell.

DOI: [10.1103/PhysRevE.87.013005](https://doi.org/10.1103/PhysRevE.87.013005)

PACS number(s): 47.27.eb, 44.25.+f

I. INTRODUCTION

A common phenomenology of turbulence is Richardson's cascade of energy transfer from large to small scales. Based on this picture, the seminal paper of Kolmogorov in 1941 [1] (K41) predicts the scaling behavior of the velocity functions $S_p(r) = \langle |\delta v(r)|^p \rangle \sim \epsilon^{p/3} r^{p/3}$ when r is in the inertial range, the range of length scales smaller than those of energy input and larger than those affected directly by molecular dissipation. Here, $\delta v(r) \equiv v(\vec{x} + \vec{r}, t) - v(\vec{x}, t)$ is the velocity difference between two points separated by a distance $r = |\vec{r}|$, $\epsilon = \langle \epsilon(\vec{x}, t) \rangle$, where $\epsilon(\vec{x}, t) = (\nu/2)[\partial_i v_j(\vec{x}, t) + \partial_j v_i(\vec{x}, t)]^2$ and ν is the kinematic viscosity of the fluid, is the mean energy dissipation rate as well as the mean energy transfer rate, and the average is taken over position \vec{x} and time t . Experiments confirmed the power-law dependence on r , but the exponent is found to be a nonlinear function of p , showing that turbulent fluctuations are intermittent.

A fundamental and yet unsettled question is how buoyancy might affect the scaling behavior in thermal convective turbulence. There are predictions [2–5] that buoyancy would give rise to a different scaling behavior for S_p and temperature structure functions R_p , first derived by Bolgiano [6] and Obukhov [7] $S_p(r) \sim (\alpha g)^{2p/5} \chi^{p/5} r^{3p/5}$ and $R_p(r) = \langle |\delta T(r)|^p \rangle \sim (\alpha g)^{-p/5} \chi^{2p/5} r^{p/5}$ for stably stratified turbulence (see Ref. [8] for a review). Here, $\delta T(r) \equiv T(\vec{x} + \vec{r}, t) - T(\vec{x}, t)$ is the temperature difference similarly defined as $\delta v(r)$, α is the volume expansion coefficient of the fluid, g is the acceleration due to gravity, and $\chi = \langle \chi(\vec{x}, t) \rangle$ is the mean thermal dissipation rate where $\chi(\vec{x}, t) = \kappa \langle |\nabla T(\vec{x}, t)|^2 \rangle$ and κ is the thermal diffusivity of the fluid. The Bolgiano-Obukhov (BO) scaling can be obtained based on a cascade of temperature variance instead of energy. A key element of the BO scaling is the thermal balance: $[\delta v(r)]^3/r \approx (\alpha g)\delta v(r)\delta T(r) \sim r^{4/5}$, which indicates that the mean rate of energy transfer is scale dependent with energy supplied by buoyancy at each scale r .

This is in contrast to Richardson's cascade in which energy is input at the largest scale only and the mean rate of energy transfer is constant in the inertial range.

The K41 scaling plus corrections due to intermittency has been observed in nonbuoyant flows. It is, thus, expected that the BO scaling would hold only when buoyancy is significant. A crossover from the K41 scaling to the BO scaling, if it does occur, should occur when the rate of change due to a velocity obeying the BO scaling is faster than the corresponding rate due to a velocity obeying the K41 scaling. Estimating the rate of change by $\delta v(r)/r$ and using the corresponding results for the K41 and BO scalings, it can be seen that the above crossover would occur when $r > L_B \equiv \epsilon^{5/4}/[(\alpha g)^{3/2} \chi^{3/4}]$, where L_B is the Bolgiano scale [8]. Using the thermal balance in the BO scaling, we see further that the power injected into the flow due to buoyancy, given by $\alpha g \delta v(r)\delta T(r)$, is balanced by the mean dissipation rate ϵ at $r = L_B$ and, therefore, for $r > L_B$, $\alpha g \delta v(r)\delta T(r) > \epsilon$. Thus, the BO scaling is expected only for $r > L_B$. For $r \leq L_B$, one expects the velocity to obey the K41 scaling and the temperature to act as a passive scalar and to obey the Obukhov-Corrsin (OC) scaling [9,10] of $R_p(r) \sim \epsilon^{-p/6} \chi^{p/2} r^{p/3}$.

A paradigm for thermal convective turbulence is turbulent Rayleigh-Bénard (RB) convection [11,12] in a fluid enclosed in a convection cell of height H , heated from below and cooled at the top. The state of fluid motion is determined by two parameters: the Rayleigh number $Ra = \alpha g(\Delta T)H^3/\nu\kappa$ and the Prandtl number $Pr = \nu/\kappa$. The BO scaling has been found in two-dimensional (2D) turbulent RB convection in direct numerical simulations with periodic boundary conditions [13] and in experiments using soap films [14] or soap bubbles [15,16]. On the other hand, the situation in three-dimensional (3D) turbulent RB convection is less clear. It has been known [17,18] that the Bolgiano scale, constructed using the energy and thermal dissipation rates measured locally, is highly inhomogeneous within the convection cell. Numerical simulations, at $Ra = 3.5 \times 10^7$ and Pr about 1, showed that [18] the height-dependent Bolgiano scale, constructed using the energy and thermal dissipation rates averaged over a cross section at different heights, is comparable to the height H at the

^{*}ching@phy.cuhk.edu.hk[†]Present address: School of Mathematics and Statistics, University of St. Andrews, St Andrews KY16 9SS, United Kingdom.

center and decreases to $0.2H$ very close to the top and bottom boundaries. Similarly, more recent numerical simulations [19] show that the local Bolgiano scale, constructed using the local energy and thermal dissipation rates measured at each position, is comparable to H except very close to the top and bottom plates of a cylindrical convection cell where it is smaller than $0.1H$ for $Ra = 1 \times 10^9$ and $Pr = 6.4$. The K41 and OC scalings (plus intermittency corrections) have indeed been observed experimentally in the central region [20], but until now, the BO scaling expected to hold near the top and bottom plates has not been observed in experiments. On the contrary, there is an experimental report [19] that the vertical velocity structure functions near the top plate obey yet a different scaling behavior predicted to hold in shear flows [21]. As a result, the validity of the BO phenomenology for turbulent RB convection has again been called into question [22].

Until now, all numerical and experimental studies have attempted to directly study the scaling behavior of the structure functions. In the earlier studies, the structure functions in the time domain were measured and the interpretation paper studied the structure functions in the time domain, and the interpretation of any scaling behavior observed in the time domain to give scaling behavior in the spatial domain is difficult in general. Only recently have direct measurements of the structure functions in the spatial domain been carried out. The reader is referred to Ref. [22] for a recent review of these earlier works. A direct study of the scaling behavior in the spatial domain is made difficult by the lack of an extended scaling behavior (this is not surprising because, even very close to the top and bottom plates, the BO scaling, if it exists, can only occur for $H > r > L_B \approx 0.1 - 0.2H$) and the presence of *a priori* unknown corrections due to intermittency to the scaling behavior.

In this paper, we show that the nature of the scaling behavior can be revealed by studying the *conditional* structure functions evaluated at given values of the locally averaged thermal dissipation rate. In Sec. II, we first derive results for such conditional structure functions based on ideas of the refined similarity hypothesis [23,24]. We find that these conditional structure functions have a power-law dependence on the value of the locally averaged thermal dissipation rate, and such dependence for the case of the BO scaling is different from the other scaling behaviors: the K41 and OC or shear-flow scalings. As a result, we can make use of this feature to reveal the BO scaling. To calculate such conditional structure functions, simultaneous measurements of velocity and temperature and the thermal dissipation rates as a function of time and space are needed. These experimental measurements are challenging and are yet to be taken. On the other hand, using available experimental measurements in 3D turbulent RB convection, we have studied the conditional temperature structure functions in the time domain using a locally averaged thermal dissipation rate that is averaged over time at the cell center and at the center of the bottom plate. We find that the dependence of these conditional temperature structure functions on the locally averaged thermal dissipation rate at the cell center is consistent with the observed K41 and OC scalings, and the corresponding dependence at the center of the bottom plate is different and reveals the BO scaling.

We discuss our analysis in Sec. III and present our results in Sec. IV. Finally, we end the paper with a conclusion in Sec. V.

II. THEORY

We use the refined similarity hypothesis [23,24] to account for intermittency corrections by replacing the average energy dissipation rate ϵ by the locally averaged energy dissipation rate $\epsilon_r(\vec{x}, t)$,

$$\delta v(r) \sim \epsilon_r^{1/3} r^{1/3}. \quad (1)$$

Here, ϵ_r is defined by

$$\epsilon_r(\vec{x}, t) = \frac{3}{4\pi r^3} \int_{B_r(\vec{x})} \epsilon(\vec{x} + \vec{y}, t) d^3 y, \quad (2)$$

where $B_r(\vec{x})$ is a spherical volume of radius r centered at \vec{x} . Equation (1) implies that $S_p(r) \sim \langle \epsilon_r^{p/3} \rangle r^{p/3}$, and the r dependence of $\langle \epsilon_r^q \rangle$, resulting from the spatial intermittency of the energy dissipation rate, would lead to corrections to the K41 scaling. The refined similarity hypothesis has been extended to temperature fluctuations by also replacing χ by the locally averaged $\chi_r(\vec{x}, t)$, which is similarly defined

$$\chi_r(\vec{x}, t) = \frac{3}{4\pi r^3} \int_{B_r(\vec{x})} \chi(\vec{x} + \vec{y}, t) d^3 y. \quad (3)$$

For passive temperature in the OC scaling [25,26],

$$\delta T(r) \sim \epsilon_r^{-1/6} \chi_r^{1/2} r^{1/3}. \quad (4)$$

For the BO scaling [27],

$$\delta v(r) \sim (\alpha g)^{2/5} \chi_r^{1/5} r^{3/5}, \quad (5)$$

$$\delta T(r) \sim (\alpha g)^{-1/5} \chi_r^{2/5} r^{1/5}. \quad (6)$$

For shear flow with passive temperature, the shear rate s introduces an additional length scale, and we have [21]

$$\delta v(r) \sim \epsilon_r^{1/6} s^{1/2} r^{2/3}, \quad (7)$$

$$\delta T(r) \sim \epsilon_r^{-1/12} s^{-1/4} \chi_r^{1/2} r^{1/6}. \quad (8)$$

We focus on the dependence on χ_r for the different kinds of scaling behaviors. For this purpose, we study the conditional velocity and temperature structure functions, defined by

$$\tilde{S}_p(r, X) \equiv \langle |\delta v(r)|^p | \chi_r = X \rangle, \quad (9)$$

$$\tilde{R}_p(r, X) \equiv \langle |\delta T(r)|^p | \chi_r = X \rangle. \quad (10)$$

Here, the average is taken under a condition, namely, only over those measurements with $\chi_r = X$. We have used such conditional structure functions [27] and similar conditional structure functions evaluated at given values of the local temperature variance transfer rate [28] or the local energy transfer rate [29] to examine the validity of the refined similarity hypothesis. Conditional statistics evaluated at a given large-scale velocity have also been used to study the effect of large-scale velocity on inertial-range turbulent statistics [30,31].

To derive $\tilde{S}_p(r, X)$ and $\tilde{R}_p(r, X)$ from Eqs. (1), (4), (7), and (8), one needs to evaluate the conditional average $\langle \epsilon_r^q | \chi_r = X \rangle$ for various values of q . In these cases, temperature is a passive scalar, thus, we can make use of the measured

approximate statistical independence of ϵ_r and χ_r for passive scalar fluctuations [32] to get

$$\langle \epsilon_r^q | \chi_r = X \rangle \approx \langle \epsilon_r^q \rangle, \quad \text{K41, shear, OC.} \quad (11)$$

As a result, we obtain

$$\tilde{S}_p(r, X) \sim \begin{cases} \langle \epsilon_r^{p/3} \rangle r^{p/3}, & \text{K41,} \\ \langle \epsilon_r^{p/6} \rangle s^{p/2} r^{2p/3}, & \text{shear,} \\ (\alpha g)^{2p/5} X^{p/5} r^{3p/5}, & \text{BO,} \end{cases} \quad (12)$$

$$\tilde{R}_p(r, X) \sim \begin{cases} \langle \epsilon_r^{-p/6} \rangle X^{p/2} r^{p/3}, & \text{OC,} \\ \langle \epsilon_r^{-p/12} \rangle s^{-p/4} X^{p/2} r^{p/6}, & \text{shear,} \\ (\alpha g)^{-p/5} X^{2p/5} r^{p/5}, & \text{BO.} \end{cases} \quad (13)$$

We note that \tilde{S}_p is independent of X for both the K41 and the shear-flow scalings and is different from the dependence of $X^{p/5}$ for the BO scaling. Similarly, \tilde{R}_p has the same power-law dependence of $X^{p/2}$ for both the OC and the shear-flow scaling behaviors, which is different from the dependence of $X^{2p/5}$ for the BO scaling. Hence, the nature of the scaling behavior could be revealed by studying the X dependence of the conditional structure functions \tilde{S}_p and \tilde{R}_p . In particular, we can distinguish the BO scaling from either the K41 and OC or the shear-flow scalings.

As discussed in Sec. I, the local Bolgiano scale $L_B(\vec{x})$, constructed using the local energy and thermal dissipation rates at each position $\epsilon(\vec{x}) = \langle \epsilon(\vec{x}, t) \rangle_t$ and $\chi(\vec{x}) = \langle \chi(\vec{x}, t) \rangle_t$ with $\langle \dots \rangle_t$ denoting an average over time t only, is highly inhomogeneous. To test the BO phenomenology in turbulent RB convection, one can calculate \tilde{S}_p and \tilde{R}_p and can study their dependence on X in two regions,

- (1) region 1: $L_B(\vec{x}) \approx H$,
- (2) region 2: $L_B(\vec{x}) \ll H$

see also Ref. [22]). A good choice for regions 1 and 2 would be around the cell center and near the top or bottom plate, respectively. It is important to choose the two regions such that $L_B(\vec{x})$ is approximately uniform within each region. In calculating $\chi_r(\vec{x}, t)$, the averaging would be taken within each region. The BO phenomenology with the refined similarity ideas, developed above, then predicts that

$$\tilde{S}_p(r, X) \sim \begin{cases} X^0, & \text{region 1,} \\ X^{p/5}, & \text{region 2,} \end{cases} \quad (14)$$

$$\tilde{R}_p(r, X) \sim \begin{cases} X^{p/2}, & \text{region 1,} \\ X^{2p/5}, & \text{region 2.} \end{cases} \quad (15)$$

III. ANALYSIS USING EXPERIMENTAL MEASUREMENTS

To calculate \tilde{S}_p and \tilde{R}_p , one needs to have measurements of velocity, temperature, and thermal dissipation rates taken simultaneously as a function of space and time. Such experimental measurements are very challenging and are yet to be performed. On the other hand, simultaneous measurements of the temperature and the thermal dissipation rate at a fixed location as a function of time have been obtained recently [33] in 3D turbulent RB convection. Using these measurements, one can calculate the conditional temperature structure functions in the time domain using a locally averaged thermal dissipation rate that is averaged over time.

The experiment was conducted in a cylindrical cell of inner diameter 19.0 and $H = 20.5$ cm, filled with water. The bulk fluid is maintained at about 30°C at which $\nu \simeq 8.2 \times 10^{-3}$, $\kappa \simeq 1.5 \times 10^{-3}$ cm²/s, and Pr is kept at $\simeq 5.5$. The range of Ra covered is $9 \times 10^8 \leq \text{Ra} \leq 9 \times 10^9$. $\chi(\vec{x}, t)$ is measured by a probe consisting of four small (0.11 mm in diameter) identical thermistors with one placed at the center and the other three placed at a distance $\delta l = 0.25 \pm 0.1$ mm from the central one, each along the three perpendicular directions. From the simultaneous temperature signals measured from the four thermistors, T from the central thermistor and T_i ($i = x, y, z$) from the other three thermistors, the three components of the temperature gradient $(T_i - T)/\delta l$ ($i = x, y, z$) and, thus, $\chi(\vec{x}, t)$ can be obtained as a function of time t . The sampling rate of the measurements is 40 Hz, and 12–30-h-long time series data at various locations in the cell were taken. Other details about the experiment can be found in Ref. [33].

Using these measurements, we have constructed [34,35] a locally averaged thermal dissipation rate, averaged over a time interval,

$$\chi_\tau(\vec{x}, t) \equiv \frac{1}{\tau} \int_t^{t+\tau} \chi_f(\vec{x}, t') dt. \quad (16)$$

Here, $\chi_f(\vec{x}, t) \equiv \kappa |\nabla T_f(\vec{x}, t)|^2$, and T_f is the temperature fluctuation. The space-time correlation functions of temperature $\langle T(\vec{x} + \vec{r}, t + \tau) T(\vec{x}, t) \rangle$ have been found [36] to depend on one variable $r_E = [(r - U_0 \tau)^2 + V^2 \tau^2]^{1/2}$, where U_0 is the mean flow velocity and V is the random sweeping velocity proportional to the root-mean-squared velocity fluctuation in accordance with a model proposed in Ref. [37]. This suggests that temperature fluctuation at the same spatial location and across a time interval τ could be related to temperature fluctuation at the same time and across a spatial distance r with $r = (U_0^2 + V^2)^{1/2} \tau$. In the same spirit, the time averaged χ_τ can be taken as the volume averaged χ_r with r and τ related by $r = (U_0^2 + V^2)^{1/2} \tau$. We note that U_0 and V could depend on r for inhomogeneous flows, such as turbulent RB convection. Such a dependence could result in a nonlinear relation between r and τ , but this would not affect the association of χ_τ with χ_r . On the other hand, a nonlinear relation between r and τ would make the relation of the scaling behavior in the time domain to that in the spatial domain nontrivial. Since we are interested in the dependence of the conditional structure functions on the value of χ_τ and not their scaling behaviors, this problem of relating the scaling behavior in the time and spatial domains is, thus, avoided.

Using the experimental measurements, we study the conditional structure functions in the time domain,

$$\hat{S}_p(\tau, X) \equiv \langle |v(\vec{x}, t + \tau) - v(\vec{x}, t)|^p | \chi_\tau = X \rangle, \quad (17)$$

$$\hat{R}_p(\tau, X) \equiv \langle |T(\vec{x}, t + \tau) - T(\vec{x}, t)|^p | \chi_\tau = X \rangle, \quad (18)$$

where the average is taken over those times at which $\chi_\tau = X$ is satisfied (in practice, the average is taken over measurements with χ_τ within a narrow range of the value X , see below for more details). The conditional structure functions, whether in spatial or time domain, have the same dimension, and χ_τ has the same dimension as χ_r , thus, \hat{S}_p and \hat{R}_p have the same power-law dependence on X as \tilde{S}_p and \tilde{R}_p ,

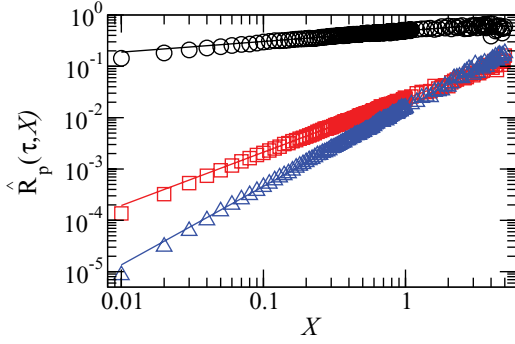


FIG. 1. (Color online) Dependence of $\hat{R}_p(\tau, X)$ on X for circles: $\tau = 108\tau_0$ and $p = 0.5$; squares: $\tau = 16\tau_0$ and $p = 2$; and triangles: $\tau = 32\tau_0$ and $p = 3$ at the cell center. The solid lines are the best fits of the power-law region.

$$\hat{S}_p(\tau, X) \sim \begin{cases} X^0, & \text{K41 or shear,} \\ X^{p/5}, & \text{BO,} \end{cases} \quad (19)$$

$$\hat{R}_p(\tau, X) \sim \begin{cases} X^{p/2}, & \text{OC or shear,} \\ X^{2p/5}, & \text{BO.} \end{cases} \quad (20)$$

Using the present experimental measurements, \hat{R}_p can be readily calculated, and we report the results in the next section.

IV. RESULTS AND DISCUSSIONS

In the calculation of $\hat{R}_p(\tau, X)$, χ_τ is measured in units of the standard deviation σ_{χ_f} of χ_f , and the average is taken over those measurements with $|\chi_\tau/\sigma_{\chi_f} - X| \leq 0.005$. To check the BO phenomenology, we evaluate $\hat{R}_p(\tau, X)$ at two locations: at the cell center at which K41 and OC scalings have been reported and at the center of the bottom plate (with one of the four thermistors touching the bottom plate) at which the local Bolgiano scale should be small compared with H . We study $\hat{R}_p(\tau, X)$ as a function of X for different values of τ (from τ_0 to $512\tau_0$ and τ_0 is the sampling time interval of $1/40$ s) and p (from 0.5 to 4). Power-law dependence on X is observed in all the cases studied, confirming the refined similarity ideas that intermittency corrections are due to fluctuations in the local thermal dissipation rate.

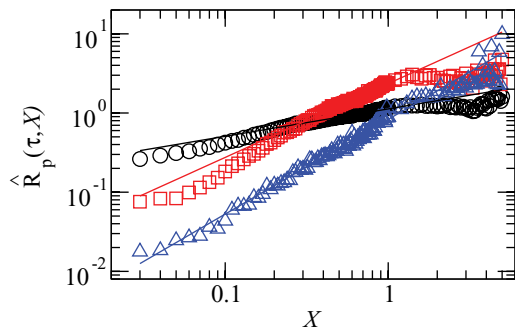


FIG. 2. (Color online) Dependence of $\hat{R}_p(\tau, X)$ on X for circles: $\tau = 45\tau_0$ and $p = 1$; squares: $\tau = 23\tau_0$ and $p = 2.5$; and triangles: $\tau = 8\tau_0$ and $p = 4$ at the bottom plate. The solid lines are the best fits of the power-law region.

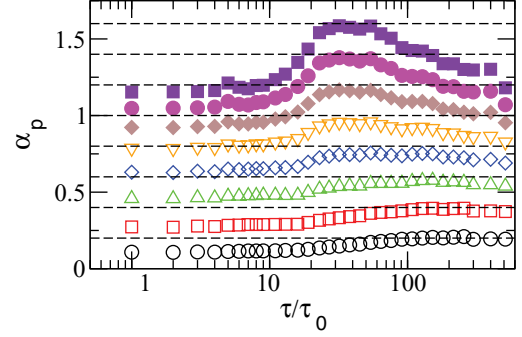


FIG. 3. (Color online) Plot of α_p as a function of τ/τ_0 for $p = 0.5-4$ in steps of 0.5 from bottom to top for measurements at the center of the bottom plate. The dashed lines are $2p/5$.

In this paper, we report results studied at $Ra = 8.3 \times 10^9$. At this Ra , σ_{χ_f} is 0.022 and 3.35 K^2/s , respectively, and the corresponding $\langle \chi_f \rangle_t / \sigma_{\chi_f}$ is 0.33 and 0.86, respectively, at the cell center and at the center of the bottom plate. Results for some values of τ and p for the two locations are shown in Figs. 1 and 2.

At each of the two locations, we choose the largest power-law region of $\hat{R}_p(\tau, X)$, common to all the values of τ and p studied. As can be seen in Figs. 1 and 2, the extent of the power laws is longer, about two decades, at the cell center and is about a decade at the bottom plate. We extract the power-law exponents, defined by $\hat{R}_p(\tau, X) \sim X^{\alpha_p}$, in this common power-law region by least-squares fit in the log-log plots. The results are shown in Figs. 3 and 4. We find that α_p depends on τ for the range of τ studied. However, the scaling behavior, whatever its nature, would hold only in a certain range of r or the corresponding range of τ , which implies that Eqs. (19) and (20) also hold only in that range of τ . For each p , α_p attains a maximum value $\alpha_m(p)$ at a certain $\tau_m(p)$, therefore, α_p is approximately constant and equal to $\alpha_m(p)$ for a small range of τ close to $\tau_m(p)$, i.e., we have

$$\hat{R}_p(\tau, X) \sim X^{\alpha_m(p)} \quad \text{for } \tau \approx \tau_m(p). \quad (21)$$

At the cell center, $\tau_m(p)$ is about $20\tau_0$ and is the same for all the values of p studied. On the other hand, it is found that, at the center of the bottom plate, $\tau_m(p)$ decreases from about $200\tau_0$ to about $20\tau_0$ as p increases, indicating that the range of τ , over which Eq. (21) holds, changes with p . This feature

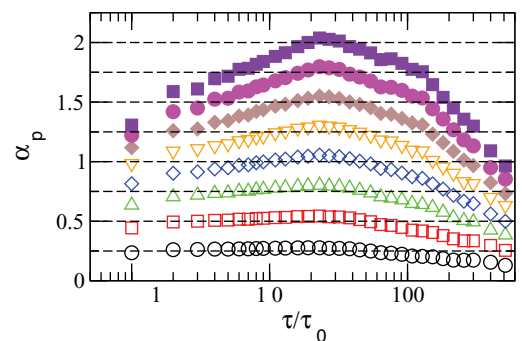


FIG. 4. (Color online) Same as Fig. 3 for measurements at the cell center. The dashed horizontal lines are $p/2$.

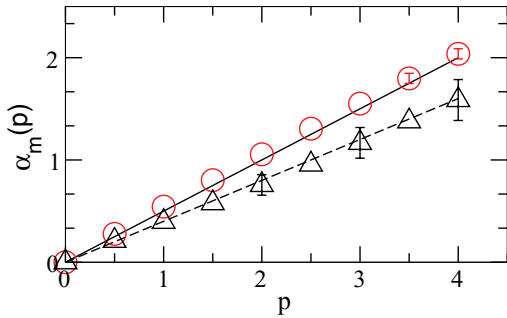


FIG. 5. (Color online) Plot of $\alpha_m(p)$ as a function of p at circles: cell center and triangles: the bottom plate. The solid line is $p/2$, whereas, the dashed line is $2p/5$.

is not clearly understood and deserves further investigation in future papers.

We plot $\alpha_m(p)$ as a function of p for the two locations in Fig. 5. It can be seen that the p dependence of $\alpha_m(p)$ is clearly different at the two locations. At the cell center, the values of $\alpha_m(p)$ are in good agreement with $p/2$ and are, thus, consistent with the experimental observation of OC scaling with intermittent corrections [20] in the central region. On the other hand, at the center of the bottom plate, the values of $\alpha_m(p)$ are in excellent agreement with the predicted values of $2p/5$ for the BO scaling. Thus, our results confirm the BO phenomenology.

V. CONCLUSION

In conclusion, we have studied the conditional velocity and temperature structure functions $\tilde{S}_p(r, X)$ and $\tilde{R}_p(r, X)$, evaluated when the locally averaged thermal dissipation rate χ_r is within a narrow range of the value X . Using ideas of refined similarity, we have derived the theoretical results that $\tilde{S}_p(r, X)$ and $\tilde{R}_p(r, X)$ have power-law dependence on X and that the power-law dependence for the BO scaling is different from the other kinds of scaling behaviors [see Eqs. (12) and (13)]. As a result, this feature can be used to reveal the nature of the scaling behavior. However, experimental measurements needed for the calculation of $\tilde{S}_p(r, X)$ and $\tilde{R}_p(r, X)$ have yet to be taken. Using available experimental measurements, instead, we have calculated the conditional temperature functions $\hat{R}_p(\tau, X)$ in the time domain, evaluated when a local thermal dissipation rate, averaged over time interval τ , χ_τ , is within a narrow

range of the value X . Since we are not studying the scaling behavior, the problem of relating scaling behavior of structure functions in the time domain to that in the spatial domain is avoided. Moreover, the X dependence of $\hat{R}_p(\tau, X)$ would be the same as that of $\tilde{R}_p(\tau, X)$, given by Eq. (20), based on dimensional analysis. We have studied $\hat{R}_p(\tau, X)$ at two locations. The first location is the cell center at which the local Bolgiano scale is comparable to H , thus, the K41 and OC scaling behaviors are expected from the BO phenomenology and have been observed experimentally. The second location is the center of the bottom plate. The local Bolgiano scale has been found to be about $0.1-0.2H$ very near the bottom plate, thus, the BO scaling behavior is expected from the BO phenomenology. The major result of our analysis of the experimental measurements is summarized in Eq. (21). This confirms the power-law dependence predicted, but our observation of $\tau_m(p)$, varying with p at the center of the bottom plate, remains to be understood. The values of $\alpha_m(p)$ that we have found at the two locations are different: At the cell center, $\alpha_m(p)$'s are consistent with the values of $p/2$ for the K41 and OC scalings at the cell center, and at the center of the bottom plate, $\alpha_m(p)$'s are consistent with the values of $2p/5$ for the BO scaling. Our results have, thus, confirmed the BO phenomenology in 3D turbulent RB convection.

Our approach of using the conditional structure functions to reveal the nature of the scaling behavior can also be applied to 2D turbulent RB convection if there is intermittency and the intermittency is caused by fluctuations of the local thermal dissipation rate. We note, however, that both intermittent velocity fluctuations [14] and intermittent temperature fluctuations [13] and nonintermittent velocity fluctuations [13,16] and nonintermittent temperature fluctuations [16] have been reported in 2D. A connection between the presence of the BO scaling and an inverse energy transfer from small to large scales, which is known to exist in 2D, has also been reported [38]. It is, thus, interesting to explore this possible connection in 3D. If an inverse energy transfer does exist, it could also explain the origin of the mean large-scale circulation present in 3D turbulent RB convection.

ACKNOWLEDGMENTS

This work was supported by the Hong Kong Research Grants Council under Grants No. CUHK-400708 (E.S.C.C.) and No. HKUST-604310 (P.T.).

-
- [1] A. N. Kolmogorov, Dokl. Akad. Nauk. SSSR **30**, 299 (1941) [reprinted in Proc. R. Soc. London, Ser. A **434**, 9 (1991)].
 - [2] I. Procaccia and R. Zeitak, Phys. Rev. Lett. **62**, 2128 (1989); Phys. Rev. A **42**, 821 (1990).
 - [3] V. S. L'vov, Phys. Rev. Lett. **67**, 687 (1991).
 - [4] V. Yakhot, Phys. Rev. Lett. **69**, 769 (1992).
 - [5] S. Grossmann and V. S. L'vov, Phys. Rev. E **47**, 4161 (1993).
 - [6] R. Bolgiano, J. Geophys. Res. **64**, 2226 (1959).
 - [7] A. M. Obukhov, Dokl. Akad. Nauk. SSSR **125**, 1246 (1959).
 - [8] A. S. Monin and A. M. Yaglom, *Statistical Fluid Mechanics* (MIT Press, Cambridge, MA, 1975).
 - [9] A. M. Obukhov, Izv. Akad. Nauk. SSSR Ser. Geog. Geofiz. **13**, 58 (1949).
 - [10] S. Corrsin, J. Appl. Phys. **22**, 469 (1951).
 - [11] E. D. Siggia, Annu. Rev. Fluid Mech. **26**, 137 (1994).
 - [12] G. Ahlers, S. Grossmann, and D. Lohse, Rev. Mod. Phys. **81**, 503 (2009).
 - [13] A. Celani, T. Matsumoto, A. Mazzino, and M. Vergassola, Phys. Rev. Lett. **88**, 054503 (2002).

- [14] Jie Zhang and X. L. Wu, *Phys. Rev. Lett.* **94**, 234501 (2005).
- [15] F. Seychelles, Y. Amarouchene, M. Bessafi, and H. Kellay, *Phys. Rev. Lett.* **100**, 144501 (2008).
- [16] F. Seychelles, F. Ingremeau, C. Pradere, and H. Kellay, *Phys. Rev. Lett.* **105**, 264502 (2010).
- [17] R. Benzi, F. Toschi, and R. Tripicciono, *J. Stat. Phys.* **93**, 901 (1998).
- [18] E. Calzavarini, F. Toschi, and R. Tripicciono, *Phys. Rev. E* **66**, 016304 (2002).
- [19] R. P. J. Kunnen, H. J. H. Clercx, B. J. Geurts, L. J. A. van Bokhoven, R. A. D. Akkermans, and R. Verzicco, *Phys. Rev. E* **77**, 016302 (2008).
- [20] C. Sun, Q. Zhou, and K.-Q. Xia, *Phys. Rev. Lett.* **97**, 144504 (2006).
- [21] D. Lohse, *Phys. Lett. A* **196**, 70 (1994).
- [22] D. Lohse and K.-Q. Xia, *Annu. Rev. Fluid Mech.* **42**, 335 (2010).
- [23] A. N. Kolmogorov, *J. Fluid Mech.* **13**, 82 (1962).
- [24] A. M. Obukhov, *J. Fluid Mech.* **13**, 77 (1962).
- [25] G. Stolovitzky, P. Kailasnath, and K. R. Sreenivasan, *J. Fluid Mech.* **297**, 275 (1995).
- [26] Y. Zhu, R. A. Antonia, and I. Hosokawa, *Phys. Fluids* **7**, 1637 (1995).
- [27] E. S. C. Ching and K. L. Chau, *Phys. Rev. E* **63**, 047303 (2001).
- [28] E. S. C. Ching and W. C. Cheng, *Phys. Rev. E* **77**, 015303(R) (2008).
- [29] E. S. C. Ching, H. Guo, and T. S. Lo, *Phys. Rev. E* **78**, 026303 (2008).
- [30] K. R. Sreenivasan and G. Stolovitzky, *Phys. Rev. Lett.* **77**, 2218 (1996).
- [31] K. R. Sreenivasan and B. Dhruva, *Prog. Theor. Phys. Suppl.* **130**, 103 (1998).
- [32] G. Ruiz-Chavarria, C. Baudet, and S. Ciliberto, *Physica D* **99**, 369 (1996).
- [33] X. He and P. Tong, *Phys. Rev. E* **79**, 026306 (2009).
- [34] X. He, P. Tong, and E. S. C. Ching, *J. Turbul.* **11**, 1 (2010).
- [35] X. He, E. S. C. Ching, and P. Tong, *Phys. Fluids* **23**, 025106 (2011).
- [36] X. He, G.-W. He, and P. Tong, *Phys. Rev. E* **81**, 065303(R) (2010); X. He and P. Tong, *ibid.* **83**, 037302 (2011).
- [37] G.-W. He and J.-B. Zhang, *Phys. Rev. E* **73**, 055303(R) (2006); X. Zhao and G.-W. He, *ibid.* **79**, 046316 (2009).
- [38] G. Boffetta, F. De Lillo, A. Mazzino, and S. Musacchio, *J. Fluid Mech.* **690**, 426 (2012).